Design and Construction of Rigs for Studying Surface Condensation and Creating Anodized Metal Oxide Surfaces

by

Wei-Yang Sun

Submitted to the Department of Mechanical Engineering
in partial fulfillment of the requirements for the degree of

Bachelor of Science in Mechanical Engineering

at the

MASSACHUSETTS INSTITUTE OF TECHNOLOGY

June 2011

Author.....
Department of Mechanical Engineering
May 16, 2011

Certified by.....
Kripa K. Varanasi
d'Arbeloff Assistant Professor of Mechanical Engineering
Thesis Supervisor

Accepted by.....
John H. Lienhard V
Collins Professor of Mechanical Engineering; Chairman,
Undergraduate Thesis Committee

Design and Construction of Rigs for Studying Surface Condensation and Creating Anodized Metal Oxide Surfaces

by

Wei-Yang Sun

Submitted to the Department of Mechanical Engineering
on May 16, 2010, in partial fulfillment of the
requirements for the degree of
Bachelor of Science in Mechanical Engineering

Abstract

This thesis details the design and construction of a rig for studying surface condensation and a rig for creating anodized metal oxides (AMOs). The condensation rig characterizes condensation for different surfaces; this is done with the use of known heat transfer principles to calculate characteristic heat fluxes and heat transfer coefficient values. Preliminary results have been shown to follow predictions derived from existing heat transfer principles, and have confirmed existing literature's assertion of increased effectiveness of dropwise condensation over filmwise condensation. The AMO rig fabricates anodized metal oxide surface samples by subjecting wafers coated with thin metal layers to voltage in the presence of acidic electrolytes. Initial fabricated anodized aluminum oxide (AAO) samples have shown to display the characteristic hierarchal nanopore structure of known fabricated AAO in literature. Both the condensation rig and the AMO rig will be used in current and future condensation and superhydrophobic surface research by the Varanasi group in the MIT Department of Mechanical Engineering.

Thesis Supervisor: Kripa K. Varanasi
Title: d'Arbeloff Assistant Professor of Mechanical Engineering

Acknowledgements

I wish to express my gratitude for the many wonderful members of the Varanasi Group who have provided to me the opportunity and the necessary resources to work on this exciting and important project. In particular, I want to give my most sincere thanks to Adam Paxson for his incredible help in producing this thesis, and to Asst. Prof. Kripa Varanasi, who, despite his long hours and busy timetable, nonetheless found time to provide invaluable guidance. Special thanks also to Mark Belanger and the Edgerton Student Shop for valuable machining resources.

Finally, I wish to thank my parents and friends, who, because of my work, would not hear back from me for days at a time; your support made this thesis possible.

Table of Contents

List of Figures

Introduction

Condensers, already implemented around the world, play vital roles in thermal-fluid systems, including those integral to energy generation and transmission. Applications of condensing systems include desalinization, solar thermal energy generation, and chemical processing. However, modern condensers contain inherent inefficiencies that can be improved in multiple ways. Most notably, they predominantly work under the *filmwise* mode of condensation, where a layer of condensed fluid forms on the condensing surface, limiting the rate of heat transfer as this insulating fluid layer thickens over time. The only literature currently in existence for improving this rate has involved minimizing the thickness of this fluid layer, but returns have been relatively low.

Dropwise condensation, on the other hand, allows fluid to condense in drops rather than in large films, which decreases overall fluid contact with the condensing surface. This in turn exposes more of this surface and results in much higher heat flux, often up to 5-7 times that of filmwise condensation [1].

Superhydrophobic surfaces are prime candidates for studies in dropwise condensation, since they by their very nature resist surface films [2]. The current challenge for widespread dropwise condensation is creating manufacturable superhydrophobic surfaces capable of withstanding the extreme conditions of industrial condensers.

Superhydrophobicity has been the subject of many recent pieces of research. Bormashenko et. al. have successfully produced and characterized metallic superhydrophobic surfaces from polymer templates [6]. However, the use of

superhydrophobic surfaces in condensation applications is not well-documented in current literature.

This thesis details the construction of two apparatus for experimental investigations in condensation surfaces, in particular those capable of condensing under the filmwise mode. The first chapter of this thesis involves the design and construction of an experimental rig for testing the condensation heat transfer coefficient on these surfaces. The second is a setup for reliably fabricating anodized metal oxide surfaces on thin metal films using known principles, but specifically in a form readily testable in the previously mentioned condensation rig.

1.1 Macroscale condensation rig

This rig will be used by the Varanasi group in various condensation studies involving examining condensation on various fabricated surfaces at operating conditions seen in typical industrial applications. These condensation effects are analyzed by calculating condensation heat transfer coefficients when condensing saturated steam onto the various surfaces. This is done by extracting heat flux through measuring thermal gradients moving away from a mounted surface sample in an controlled steam environment. This controlled environment, as well as the sample itself and the rig's installed thermal instruments and pipe fittings, is contained in a vacuum chamber, which constitutes the main body of the condensation rig. The construction of the rig, as well as preliminary runs and future steps, are outlined in this first chapter.

1.2 Anodized metal oxide (AMO) fabrication rig

This AMO rig was originally commissioned by members of the Varanasi group This research strives to study one family of surfaces in particular – *anodized aluminum oxides* (AAO). By applying electric current to an aluminum film under certain conditions, characteristic hierarchal nanostructures consisting of small deep pores can be created – these surface structures have been shown to exhibit superhydrophobicity [3].

Many reasons exist for studying AAO: not only does it exhibit incredible wetting resistance and can be easily grown from metal films on standard silicon wafers [4], but it also has large-scale manufacturing potential. Furthermore, it is relatively straightforward to adapt existing AAO fabrication methods, since different procedures for creating AAO are well-documented [7].

To study the AAO surfaces, a condensation rig was designed and fabricated. Samples prepared in the AAO rig were mounted in the condensation rig, where condensation heat transfer properties were examined.

1.3 Nomenclature

h_c	condensation heat transfer coefficient
k_{Cu}	thermal conductivity of copper
k_{In}	thermal conductivity of indium
k_{Si}	thermal conductivity of silicon
q''	normalized heat flux of condensation
R_{cont}	contact thermal resistance at indium foil interfaces
R_{In}	conductive thermal resistance through indium foil

R_{Si}	conductive thermal resistance through silicon wafer
T_{Cu}	temperature of copper cooling block (function of x)
T_s	temperature at silicon wafer sample
T_{sat}	temperature of saturated water vapor environment
V	volume of droplet on flat condensing surface
w_{Si}	thickness of silicon wafer
w_{In}	thickness of indium foil
x	distance along wafer axis into copper block

1 Condensation Rig

1.1 Survey of previous experiments

In the past, studies of dropwise condensation have been conducted on non-superhydrophobic materials, such as PTFE-coated [8] and oleic acid-promoted copper [9].

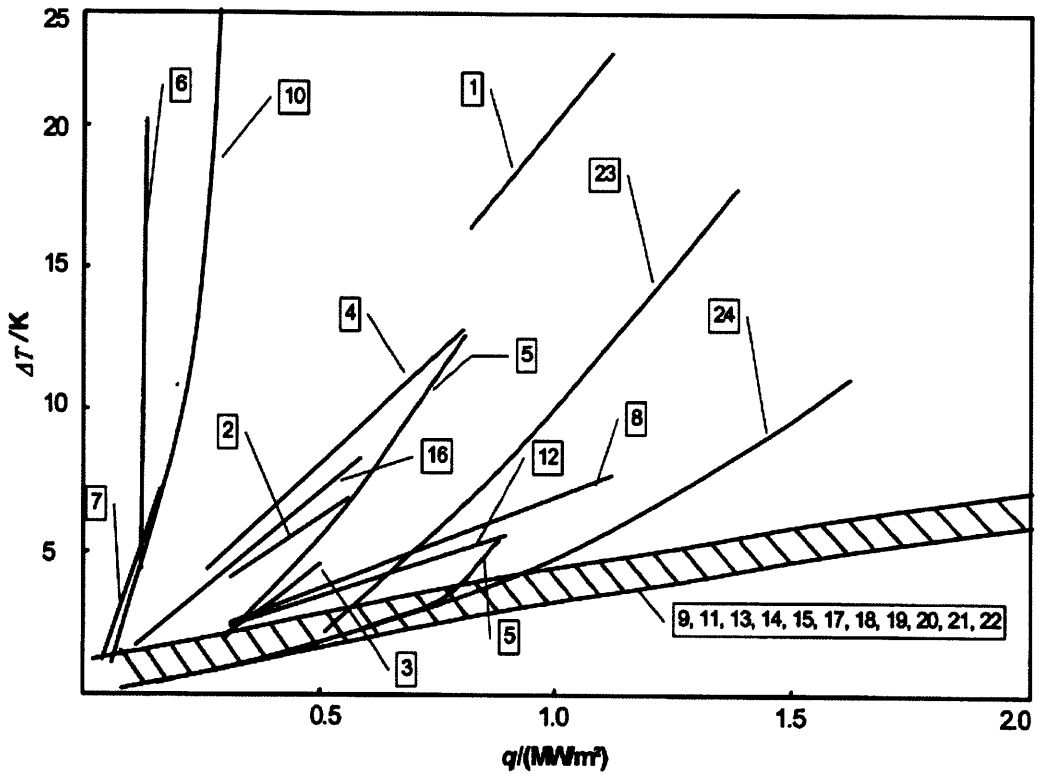

Figure 1-1: (*Figure reproduced from Rose 2002 [1]*) Heat transfer measurements for dropwise condensation of steam at near-atmospheric pressure: 1, Schmidt et al. (1930); 2, Nagle et al. (1935); 3, Gnam (1937); 4, Fitzpatrick et al. (1939); 5, Shea and Krase (1940); 6, Fatica and Katz (1949); 7, Kirschbaum et al. (1951); 8, Hampson and Ozisik (1952); 9, Wenzel (1957); 10, Welch and Westwater (1961); 11, Le Fevre and Rose (1964); 12, Kast (1963); 13, Le Fevre and Rose (1965); 14, Tanner et al. (1965a); 15, Citakoglu (1966); 16, Griffith and Lee (1967); 17, Citakoglu and Rose (1968); 18, Graham (1969); 19, Wilmshurst and Rose (1970); 20, Tanasawa and Ochiai (1973); 21, Aksan and Rose (1973); 22, Stylianou and Rose (1980); 23, Ma et al. (1994); 24, Leipertz and Koch (1998).

1.2 Overview of Condensation Rig

To study condensation at conditions seen in typical power and desalination plants, we designed and constructed an apparatus that would condense onto macroscale samples with characteristic dimensions of many centimeters. At this scale, droplet shedding plays a large role in the augmentation of the condensation heat transfer coefficient. The rig employs a modular design that enables various configurations of sample surfaces to be inserted into the condensing chamber. This portion of the study focuses on condensation onto flat surfaces with varying orientations. Future work will involve condensation onto tube configurations.

At its most fundamental level, the condensation apparatus is analogous to a typical steam cycle power plant. Instead of a fuel-fired boiler, it uses an electric boiler to introduce saturated steam into a chamber that is held at sub-atmospheric pressures. A feedback-controlled pressure regulator takes the place of steam turbines in the apparatus. A substrate is attached to a cooling block and exposed to the saturated steam, initiating heterogeneous condensation. By measuring the temperature at precise locations within the apparatus, we can calculate h_c, the condensation heat transfer coefficient.

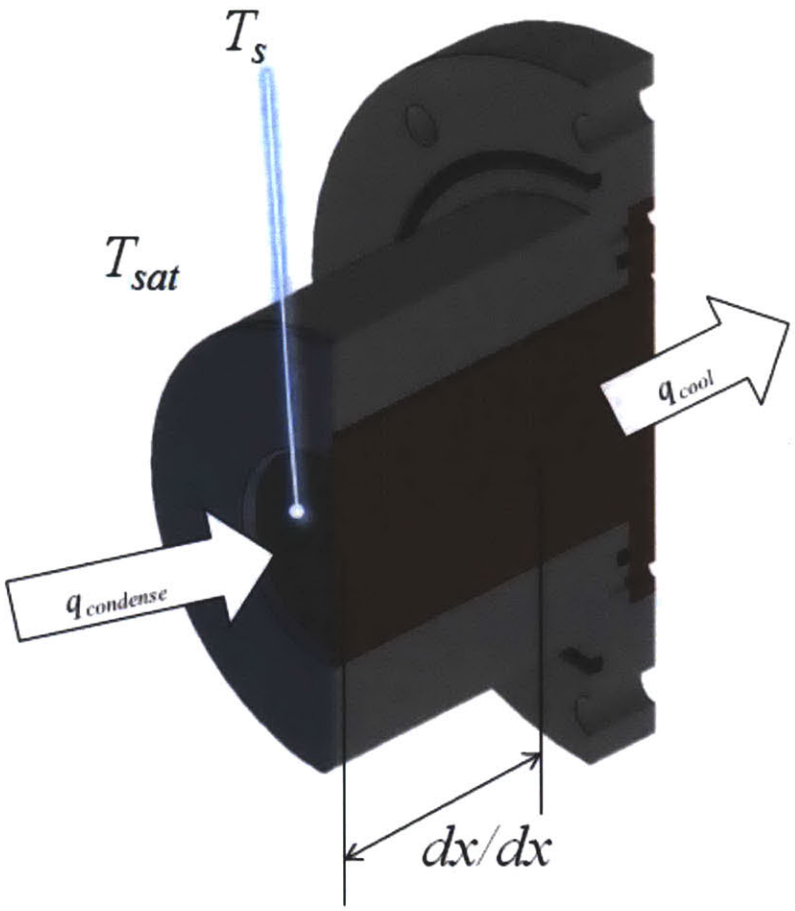

Figure 1-2 A side cross-section view of the copper cooling block in PTFE insulation. The retaining ring presses the sample wafer against the cooling block, compressing the indium thermal interface foil and increasing condensation. The equally-spaced thermocouples within the block (holes shown) measure the temperature gradient, which is important in determining h_c.

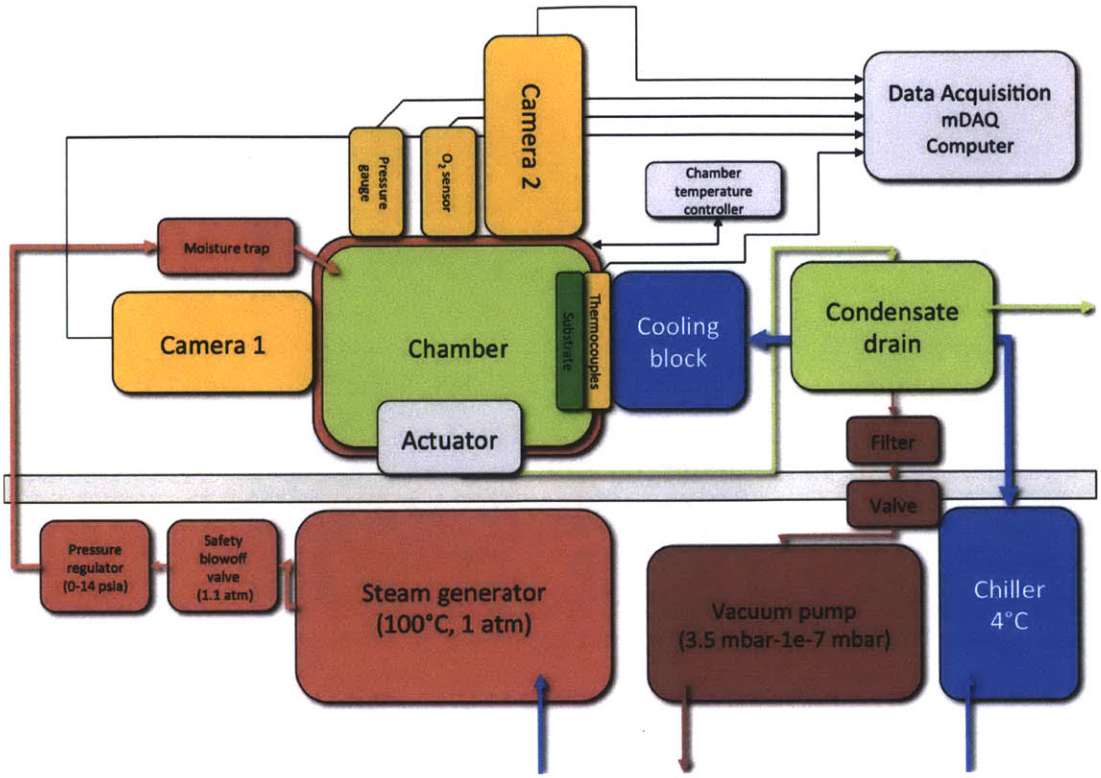

Figure 1-3: A system diagram of the condensation rig.

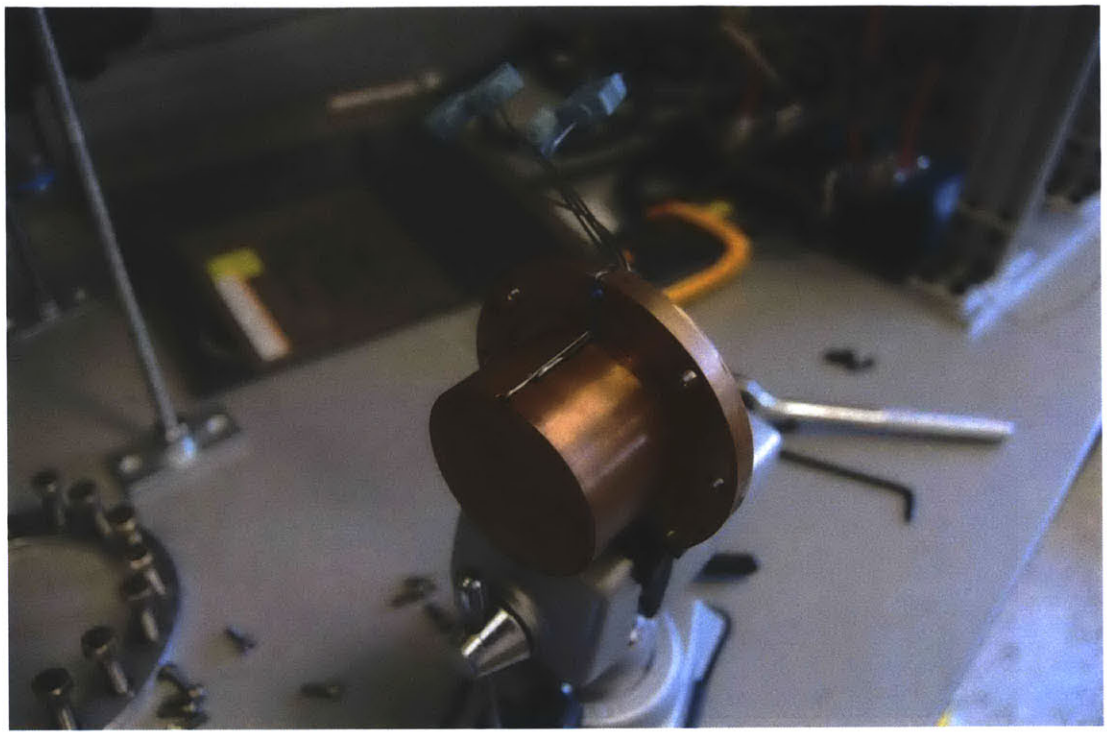

Figure 1-4: Photograph of copper cooling block, with thermocouples visible. The ends of these thermocouples extend to the central axis of the block.

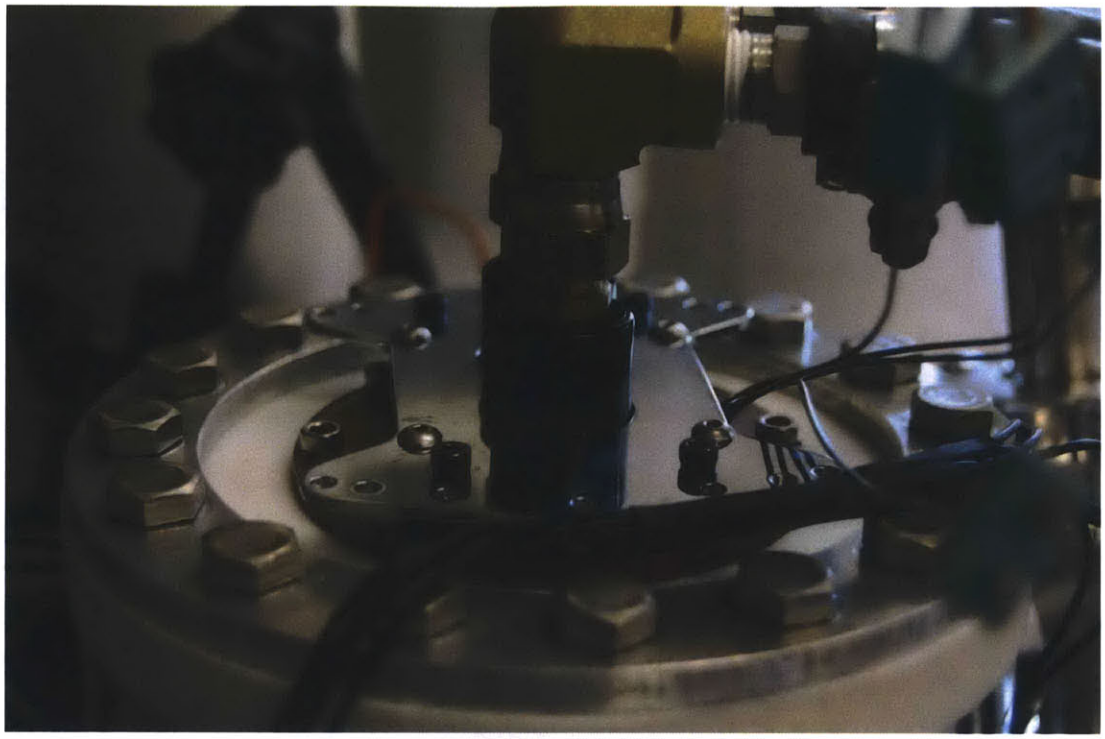

Figure 1-5: The copper block from Figure 1-4 in the chamber, mounted in PTFE insulation and with chilled water feed lines attached. Inside the chamber, on the internal-facing side of the block is mounted a condensation surface sample, which is exposed to steam when saturated vapor is introduced into the chamber.

A copper cooling block, upon which a condensation sample is attached, is subjected simultaneously to a high-temperature steam environment, and a low-temperature chilled water supply; this results in heat flux from the front to the rear of the cooling block. Temperatures within the block follow a linear profile, as dictated by Fourier's law of conduction. [11]

$$q'' = k_{Cu}\frac{dT_{Cu}}{dx} \qquad 1$$

Using the four thermocouples installed in the copper block, one can obtain the slope of this linear profile necessary to calculate the heat flux q''. The thermal

resistances in figure are all arranged in series; therefore, the heat flux through the entire system of resistance is equal.

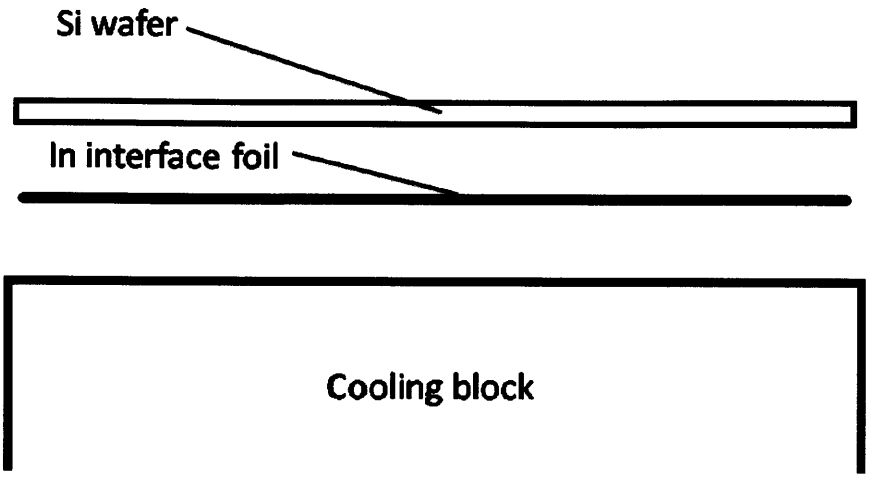

Figure 1-6: A side-view diagram of the silicon wafer, indium interface foil, and copper cooling block. When the condensation rig is in operation, the three layers are pressed firmly together by the retaining ring.

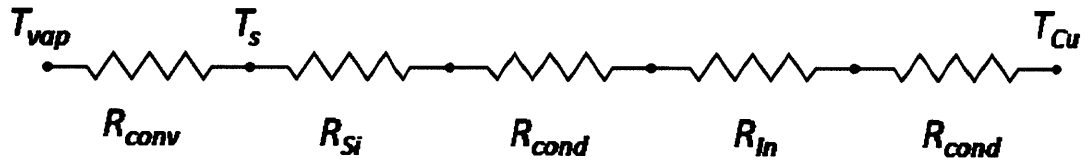

Figure 1-7. The thermal resistance diagram of the elements described in Figure 1-6, between the vapor environment and the surface of the copper cooling block, encompassing (from the left) the resistance due to convection, the conductive resistance of the silicon wafer, the resistance between the wafer and the indium foil, the conductive resistance of the indium foil itself, and the resistance between the foil and the cooling block surface.

In this study, because all thermal resistances are placed in series, we assumed that q'' is also the heat flux at the interface between the steam environment and the sample, and is in fact the heat flux at any point between the condensing surface and the rear of the cooling block.

The conductive thermal resistances of silicon and indium are defined as follows:

$$R_{Si} = \frac{w_{Si}}{k_{Si}} \quad (2)$$

$$R_{In} = \frac{w_{In}}{k_{In}} \quad (3)$$

Following the resistance diagram (Figure 1-7. The thermal resistance diagram of the elements described in Figure 1-6, between the vapor environment and the surface of the copper cooling block, encompassing (from the left) the resistance due to convection, the conductive resistance of the silicon wafer, the resistance between the wafer and the indium foil, the conductive resistance of the indium foil itself, and the resistance between the foil and the cooling block surface.), the thermal resistances between the copper surface and the silicon wafer surface exposed to the steam environment was obtained. The combined thermal resistance and the heat flux obtained via equation (1) yields the temperature difference between the sample and the surface of the copper cooling block:

$$T_s - T_{Cu}(0) = q''(R_{Si} + 2R_{cont} + R_{In}) \quad (4)$$

where R_{cont} is the thermal contact resistance at the two indium foil interfaces (provided for different clamping pressures by the indium foil

manufacturers). By combining equations (2), (3), and (4), the temperature at the sample was calculated:

$$T_s = T_{Cu} + q''(\frac{w_{Si}}{k_{Si}} + 2R_{cont} + \frac{w_{In}}{k_{In}}) \quad 5$$

This allows for the calculation of the condensation heat transfer coefficient h_c, which characterizes a surface sample's effectiveness of condensation. This h_c is defined by Newton's law of cooling, is defined as

$$h_c = \frac{q''}{T_{sat} - T_s}. \quad 6$$

1.3 Design of Rig

The main body of the condensation rig consists of a vacuum chamber, which can be easily rotated 90° on its base via a worm gear, effectively tilting the condensation surface anywhere between fully horizontal and fully vertical. This allows the examination of variable droplet roll-off angles' effects on condensation efficiency.

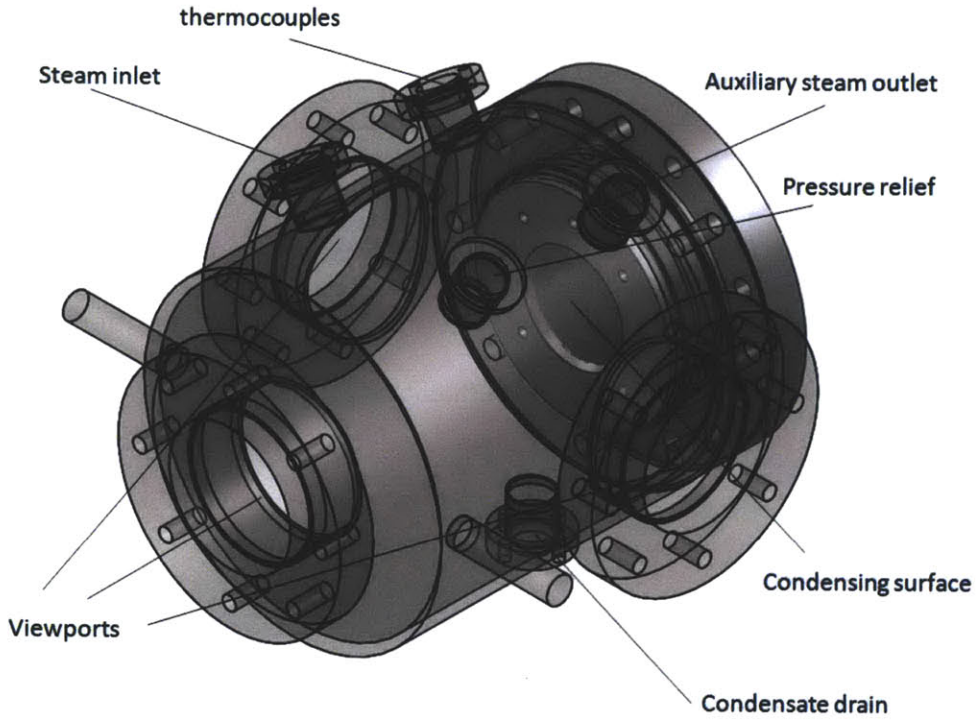

Figure 1-8: An annotated diagram of the condensation rig's main chamber.

Saturated steam is introduced into the main chamber via an electric steam generator, which generates vapor from highly-pure water. An installed moisture trap ensures that only saturated vapor enters the chamber. The pressure within the chamber is maintained at desired values using a feedback-control pressure regulator.

The main functional center for studying surfaces' condensing properties is located at one end of the chamber. There, a surface to be studied (on a silicon wafer substrate) is mounted on a copper cooling block. The silicon wafer is clamped onto a copper cooling block, which is mounted in PTFE insulation. The wafer was clamped onto the cooling block using a retaining ring, also composed of PTFE for its thermal

insulating and material properties, so that heat transfer through the indium interface foil (situated between the wafer and the cooling block) is optimized through compressive force, which increases surface contact.

The copper cooling block contains four equally-spaced thermocouples, which reach down to the cooling block's center axis (Figure 1-2 and Figure 1-4). These thermocouples allowed accurate temperature readings within the copper, which were used to calculate the heat flux through the sample, and thus determine the effectiveness of the condensing surface. The cooling block is attached to a cooling system, which keeps the temperature of one end of the copper block low using continuously-supplied chilled water.

The chamber was designed to operate to high vacuum (~2 psi); this was necessary to evacuate the condensation surface's sample environment of noncondensables (nitrogen, oxygen, etc.), so that only pure saturated steam is exposed to the sample. To this end, stainless steel was chosen as the main chamber material, and viewports rated for ultra high vacuum were chosen.

Four feedthroughs are positioned at the top of the chamber. The first one allows access for a thermocouple module that measures the temperature of the saturated vapor environment. The second one serves as the steam inlet, which introduces saturated steam from the boiler. The third feedthrough is the steam outlet, which leads to a vent leading away from the laboratory, and also provides the means for controlling the pressure within the chamber – this was done by varying the flow through a needle valve and tracking the values from the pressure transducer. There

also exists a fifth feedthrough, positioned at the bottom of the chamber, which serves as a condensate drain.

Three viewports are positioned at three different points on the chamber, providing a head-on view of the surface sample as well as two side views to the left and right of the sample. One of the side viewports may be used to introduce light into the chamber for easier viewing, photographing, and filming.

While condensation on the studied surface sample is desired, condensation on any other surface in this rig is not; excess condensates make tedious condensate draining more frequent, and can accelerate damage of piping components. In addition, secondary condensation on the viewports obstructs the view, which negatively affects the operator's ability to observe the sample. To remedy this issue, band heaters were installed on the external surfaces of both the main chamber body and the viewports. Through temperature controllers and thermocouples attached to both the chamber and viewports, these band heaters' temperatures are maintained at temperatures above the saturation point of the condensing runs, greatly reducing unwanted condensation.

A chilled water supply is connected to the rear external end of the copper cooling block, feeding and returning chilled water. This supply is also connected to a heat exchanger, which serves to cool down drained condensates from the chamber.

An electric boiler was used to provide steam for the chamber. A DI water supply serves as the water source for the boiler. This steam first meets a moisture trap before being introduced into the chamber, ensuring a stream consisting of liquid-free saturated steam. A condensate collector removes liquid water from the steam

outlet before outgoing gases are allowed to enter the laboratory's vacuum system; excess liquid water entering the vacuum inlet would otherwise result in damage.

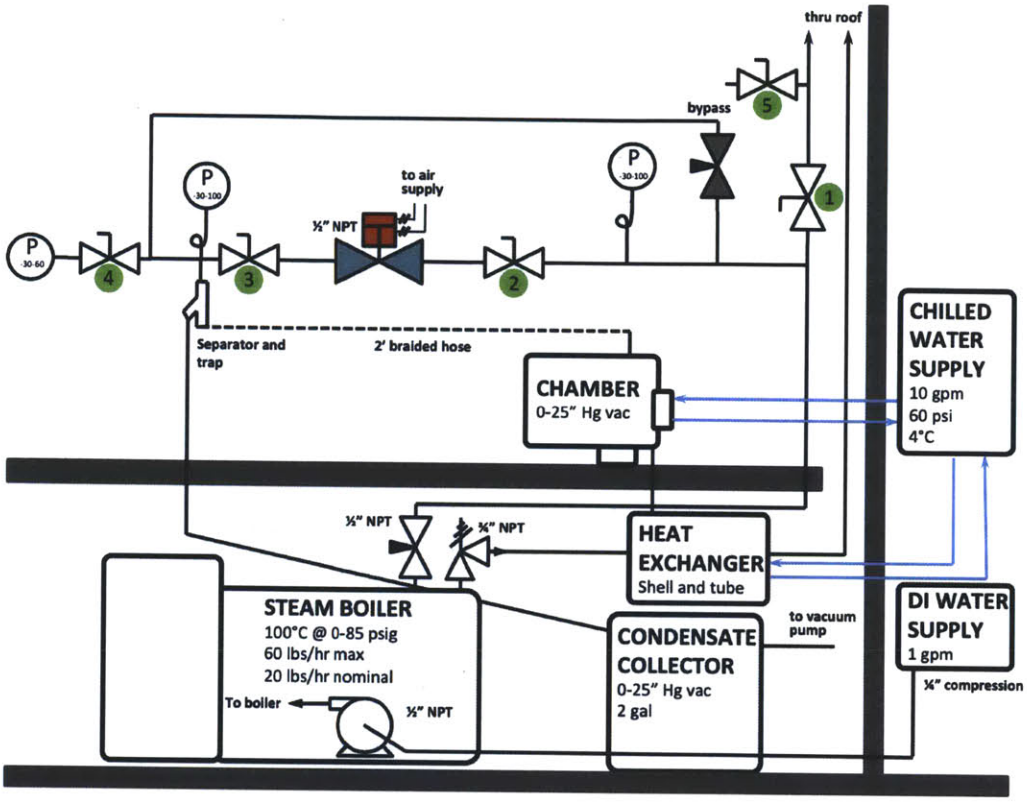

Figure 1-9: A diagram of the condensation rig piping layout.

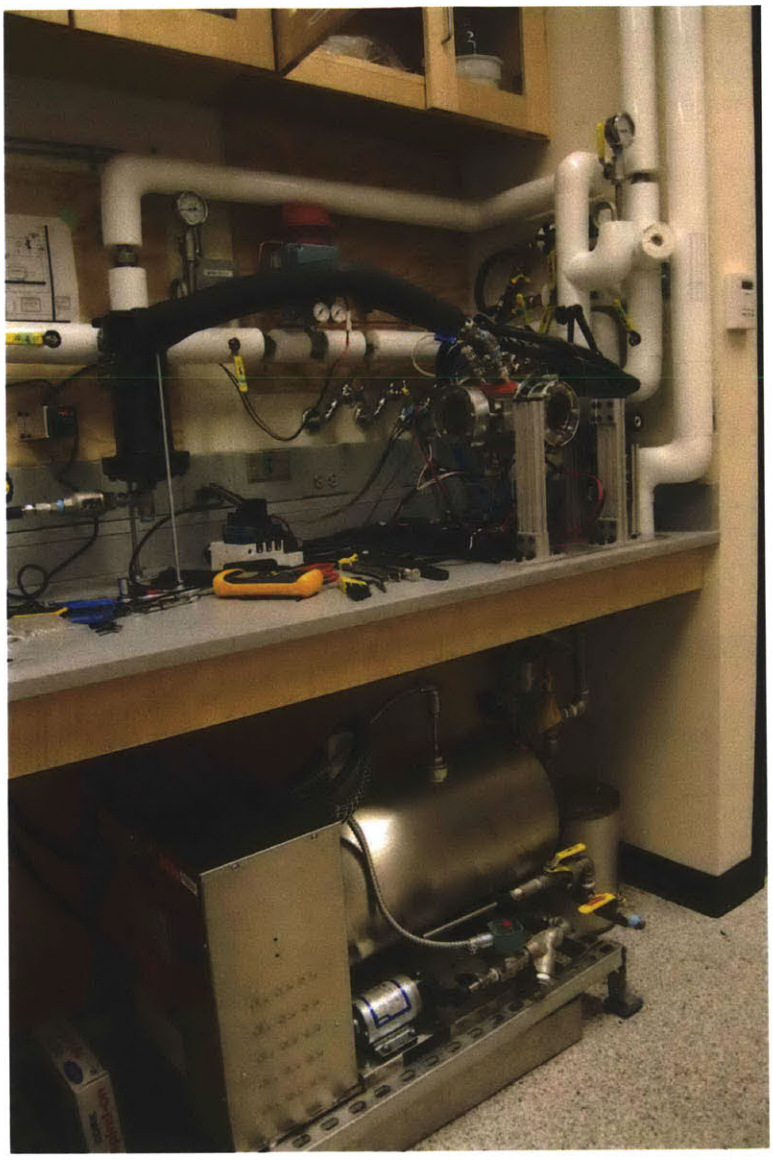

Figure 1-10: A photograph of the complete condensation rig setup. Here, many of the main components, as described in the piping layout (Figure 1-9) are visible.

The copper block thermocouple values, as well as the temperature of the steam within the chamber, were sent to an NI data acquisition module and the processed on a computer using LabVIEW code. The LabVIEW code then used this information to calculate the condensing heat transfer coefficient (Equation 6).

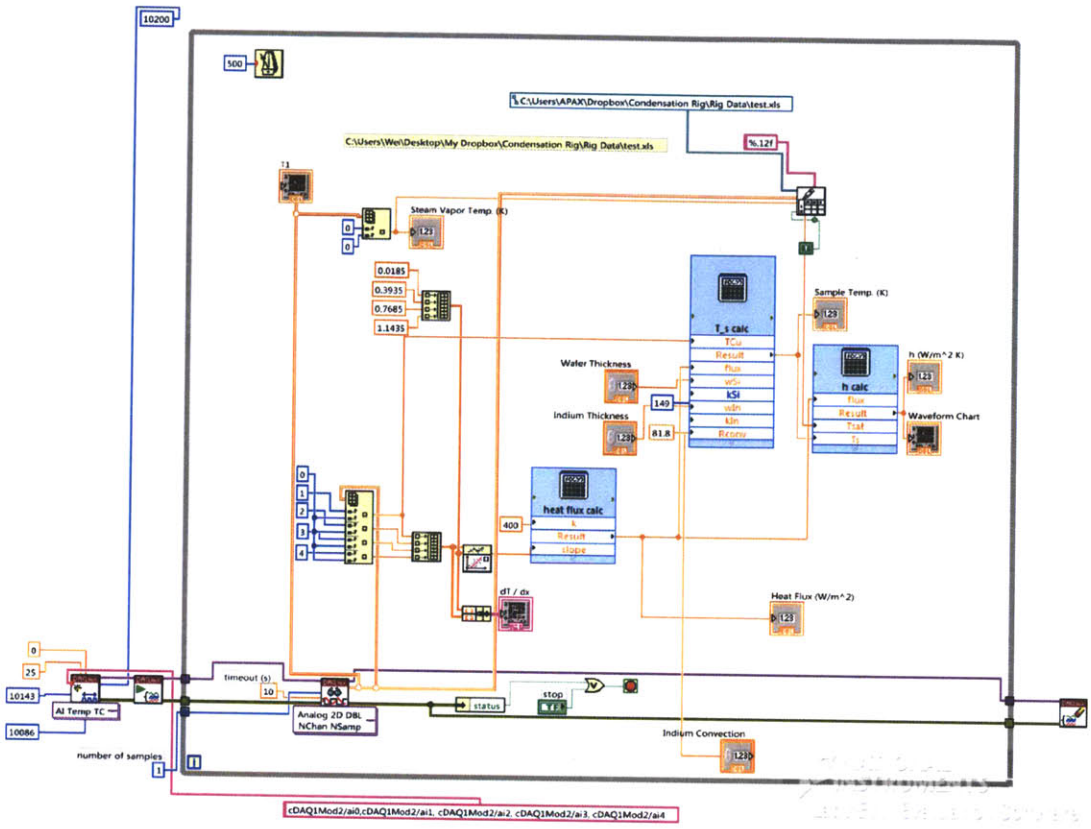

Figure 1-11: Block diagram of LabVIEW code used to analyze condensation rig data.

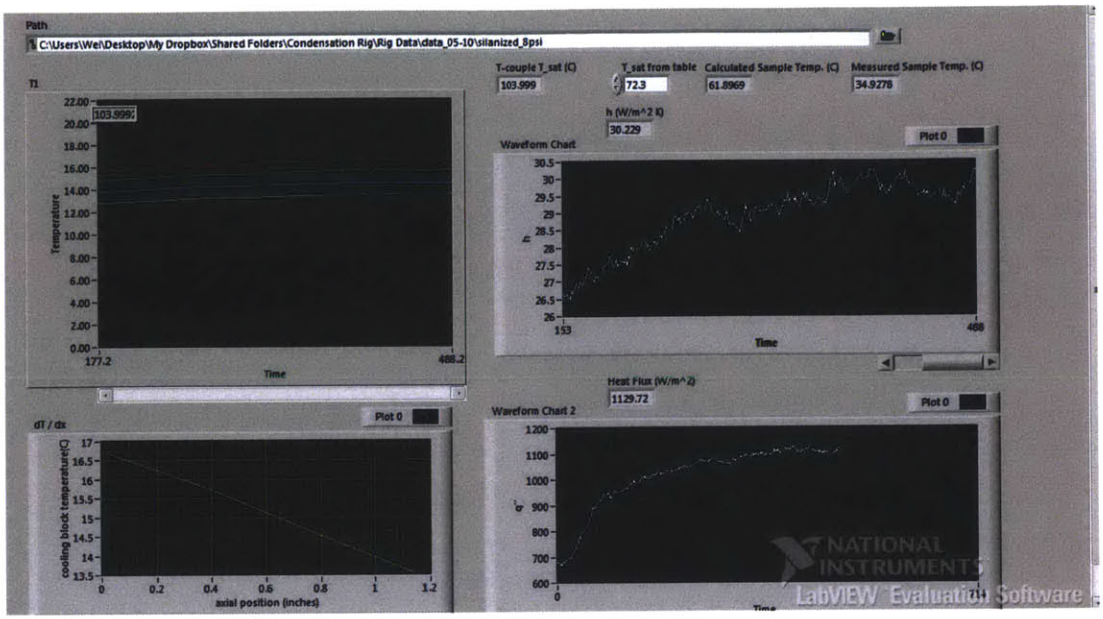

Figure 1-12: LabVIEW front panel for analyzing condensation rig data. The display windows show (counterclockwise from top left) the 4 cooling block thermocouple temperature traces over time, the same traces as a function of axial distance from the cooling block surface, the heat flux, and the calculated heat transfer coefficient of condensation.

1.4 Next Steps

The condensation rig will continue to be of great use to the Varanasi group in the future. While the rig is fully functional now, there still are many possible improvements that can be implemented.

Currently, the regulation of the pressure within the chamber is handled manually; eventually, an electronic pressure control valve can be installed to regulate the pressure via feedback control.

There is currently a minor concern that readings taken from the rig are affected by the band heaters installed on the chamber body and the viewports. Conduction

from the heaters to the sample and cooling block should be investigated in more detail to characterize their influences on obtained data.

1.5 Results

To provide a first pass comparison of dropwise versus filmwise condensation, we created a sample that was half bare silicon wafer and half fluorosilanized silicon wafer. To create this sample, fluorosilane was deposited in vapor phase in a vacuum dessicator, and half of the wafer was masked to prevent silanization.

Figure 1-13: 10 microliter water droplets on each side of 50/50 bare silicon and fluorosilane surface. The contact angle on the bare silicon side (top) was 10 +/- 2 degrees, and the contact angle of the fluorosilanized surface (bottom) was 122 +/- 2 degrees. Contact angles were measured on a Ramé-aart Model 500 Advanced Goniometer with DROPimage Advance v2.4 software.

This wafer was then mounted on the condensing surface stage within the chamber, and the condensation was observed. The juxtaposition of the two different surfaces made the differences in condensing behavior on each side readily apparent. This confirms that silicon wafer with vapor-deposited fluorosilane condenses in the dropwise mode, while bare silicon operates in filmwise mode.

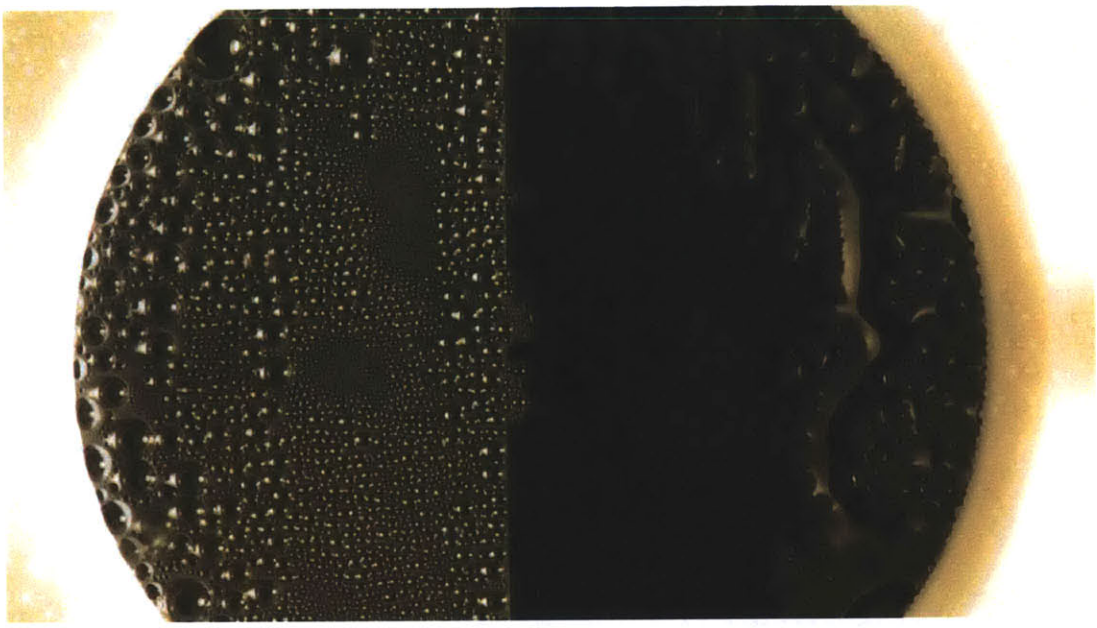

Figure 1-14: Condensing run for the fluorosilanized/bare silicon wafer sample.

To demonstrate that this condensation works as specified, i.e. allow users to characterize heat transfer properties of different condensing surfaces, three different surfaces in 2-inch rig-ready form factors were prepared: a plain unmodified silicon wafer (representing filmwise condensation), a fluorosilanized silicon wafer (dropwise), and a very rough preliminary anodized aluminum sample (2" x 1/16" aluminum plate anodized in the AMO rig, described in the next chapter). Condensation data was extracted at an absolute chamber pressure of 11 psi

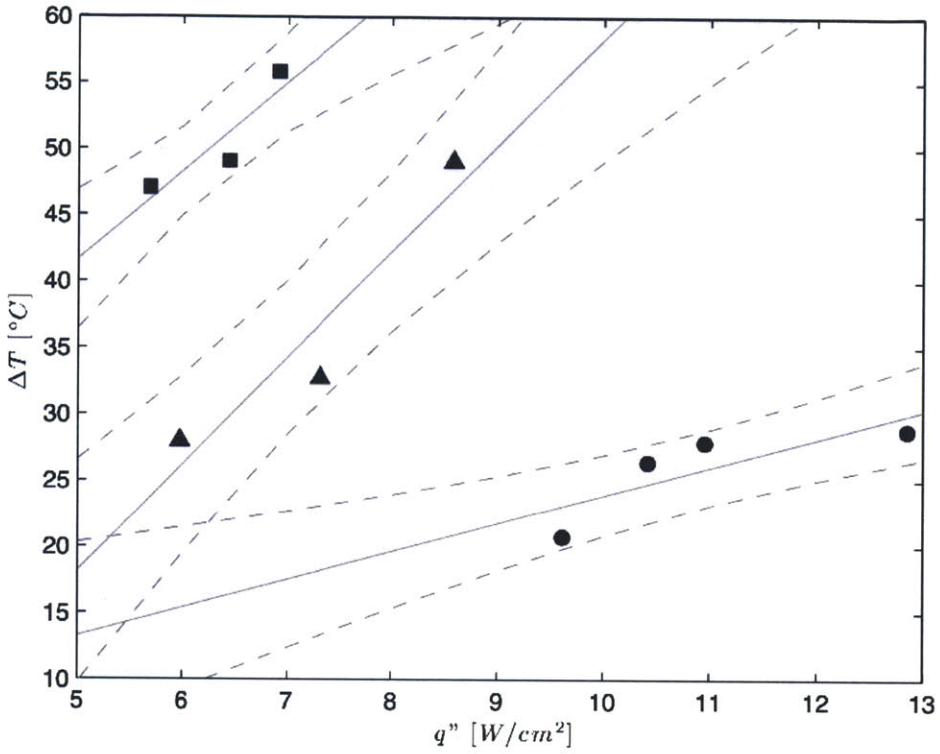

Figure 1-15: A plot of initial condensation rig results obtained, with regions representing 95% confidence bounds for three different surfaces: anodized aluminum oxide (squares), bare silicon (triangles), and fluorosilanized silicon (circles).

The data followed expected trends; the dropwise fluorosilanized silicon wafer yielded higher heat flux than filmwise bare wafer for smaller increases in surface/environment temperature difference. The preliminary AAO also performed as expected; the rough process and surface features result in many pits and other imperfections that increased droplet pinning. These preliminary runs were a success, for they validate the physical concepts that the design of the rig exploited to quantifiably study condensation on surfaces. This demonstration ensures the continued long-term use of this rig in many future condensation surface projects.

2 AMO Rig

2.1 Macroscale Wetting and Adhesion

Droplet adhesion on surfaces is characterized by their contact angle, which is the angle between a droplet's liquid-vapor interface and the solid surface. In general, surfaces with droplet contact angles below 90° are termed hydrophilic, while those contact angles greater than 90° are labeled hydrophobic.

The surface is said to exhibit superhydrophobicity when it is particularly difficult to wet; more specifically, the contact angle of a static droplet must be higher than 150° [5].

Surface features (roughness features) are necessary to achieve superhydrophobicity. Two types of droplets can be observed on such surfaces – Cassie (non-wetting) and Wenzel (wetting). A droplet in Wenzel state fully wets the surface features below it, making the droplet unable to slide across the surface and causing the droplet to exhibit high contact angle hysteresis. However, a droplet in Cassie state makes contact with the surface without wetting (the droplet does not impregnate the surface features), allowing for easy roll-off of the droplet. Dropwise condensation requires prevalence of the Cassie state to achieve heat flux improvements via rapid droplet shedding.

2.2 Anodized aluminum oxide procedure

This AMO rig was originally designed to perform the two tasks necessary to fabricate anodized aluminum oxides on a substrate: anodizing (pore initiation and oxide growth. creating the preliminary AAO structure and height), and postetching (which gradually etches the preliminary sample, for producing wider pores or

posts). In the AAO rig, corrosion-resistant platinum wire is suspended above the wafer sample, and the wafer itself is pressed into a copper base below. A strong acid solution is poured into the main cavity, submerging the top surface of the wafer sample and the lower portions of the platinum wire. Wire leads from a voltage source are attached to both the platinum wire and the copper base, completing a circuit encompassing the voltage source, platinum wire, acid solution, aluminum film with silicon wafer substrate, and copper base. Applying a voltage either anodizes this aluminum film or widens the pores, depending on which acid is used and with which time and voltage parameters, creating AAO's characteristic nanoarray aluminum oxide structure on the silicon wafer.

After the anodizing process for each sample, fluorosilane was applied. Fluorosilane can be applied either from a solution or from vapor – both were studied for their respective effects on AAO's effectiveness as a condensing surface.

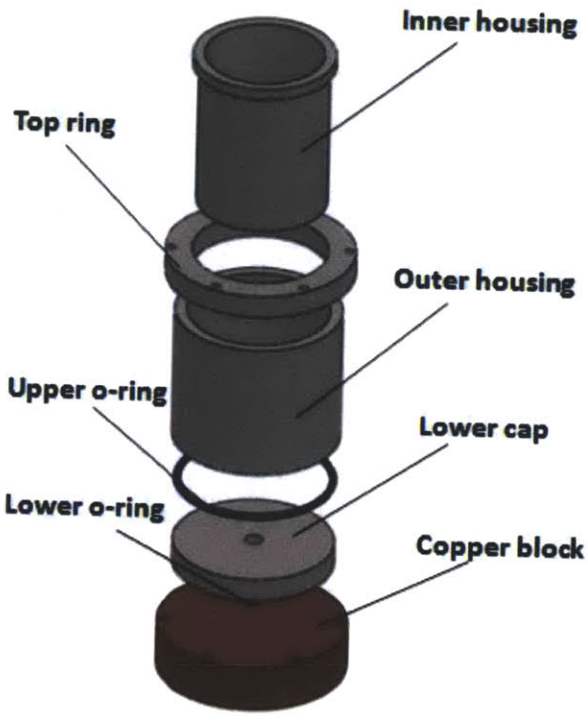

Figure 2-1: Exploded view of AAO rig.

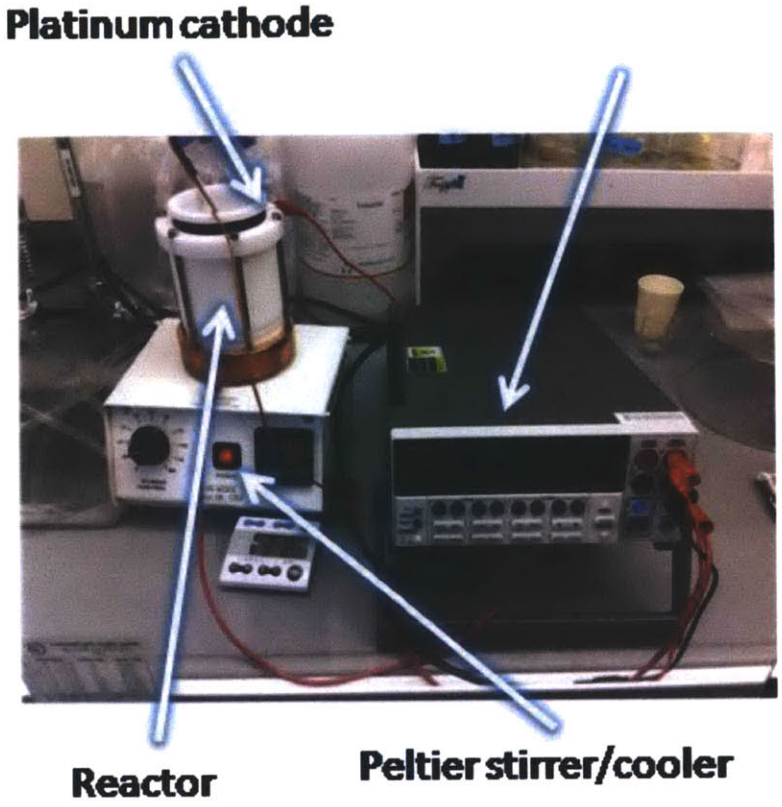

Figure 2-2: Annotated photograph of AAO rig in use. The main body of the rig is placed on a Peltier cooler/stirrer, and electrical leads from the platinum wire and copper base are connected to a Keithley 2400 SourceMeter, which provides a voltage through the rig. This setup is used for both anodizing and postetching.

2.3 Results

Preliminary AAO fabrication runs have been very promising, from the very first rough anodizing run with regular aluminum foil. From these first samples, characteristic honeycomb structures were already observed.

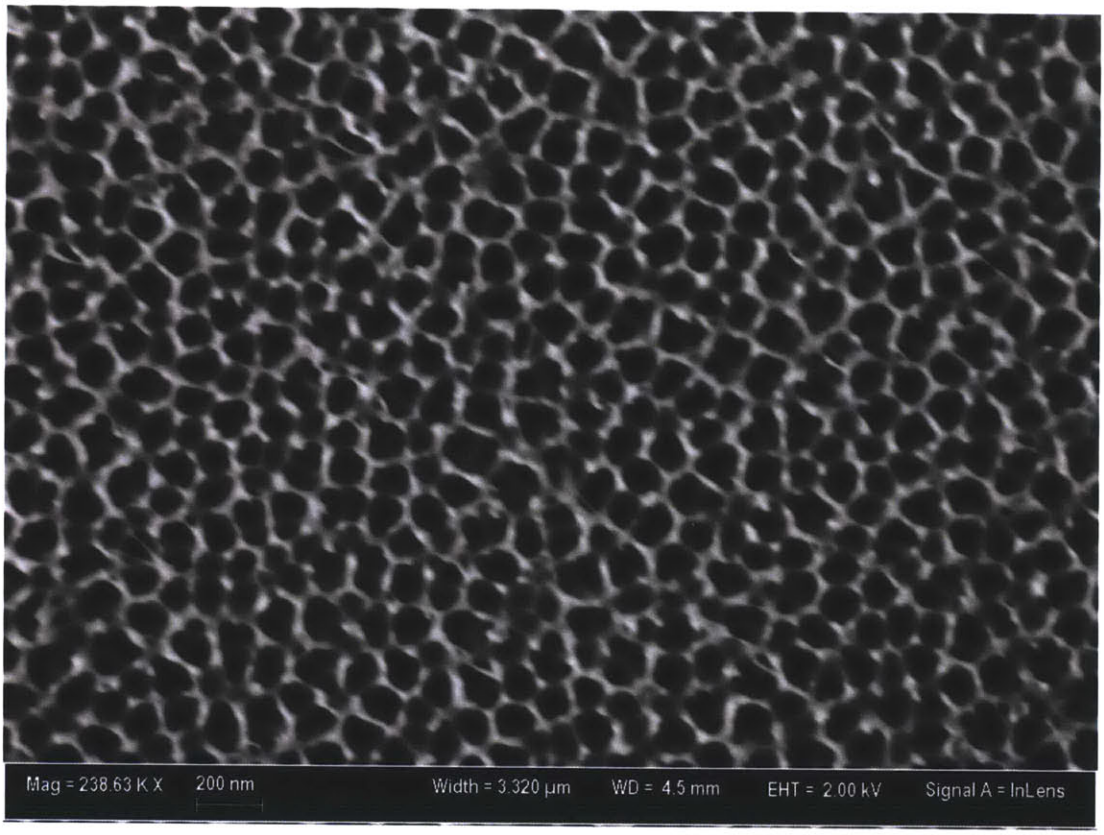

Figure 2-3: SEM image of the characteristic honeycomb nanostructure of an anodized sample, created in the AAO rig.

By varying the time periods over which the growth and postetching steps are executed, long pores and thin walls or posts can be created, allowing for great variability in fabricated AAO samples. This follows previously-observed AAO formation in other laboratories [8].

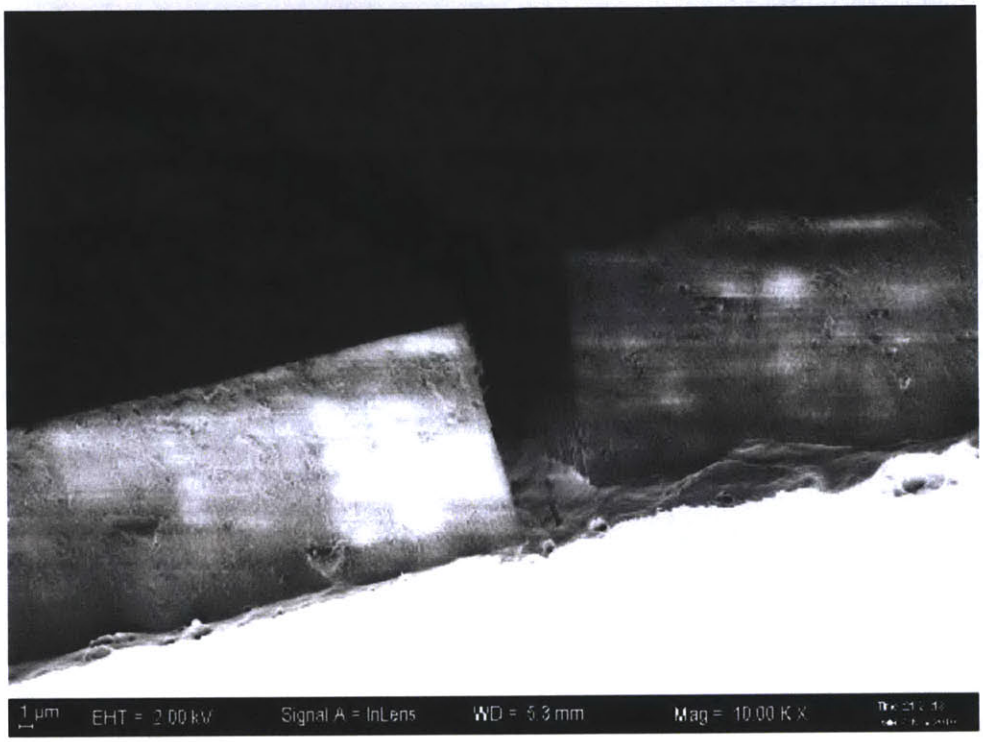

Figure 2-4: A side view SEM image of an initial fabricated sample, created in the anodization rig.

Similar processes can be applied to create other metal oxides of hierarchal nanostructure, such as anodized titanium oxide (ATO), another candidate for superhydrophobic industrial condensation applications. This rig will enable the fabrication of these condensation surface samples as well, which can then be characterized in the condensation rig outlined in the first chapter.

3 Conclusion

A robust rig to study condensation in conditions similar to those in industrial settings was designed and built using heat transfer principles. Preliminary test runs in this rig show great promise, and the rig has been found to very effectively induce condensation, produce meaningful data, and allow viewing of the processes involved. This rig will aid important work in characterizing different condensation surface candidates.

A rig to fabricate anodized aluminum oxide surface samples in the lab was created in accordance with known methods of growing and postetching characteristic AAO surfaces. AAO is known to withstand industrial conditions of high pressures and temperatures well, and has also been shown to have superhydrophobic characteristics, making this surface a strong possible candidate for industrial dropwise condensation.

These two apparatus will be of great use in future studies, especially in conjunction with one another; AAO samples created at varying parameters can be characterized in the condensation rig. This direction of study can eventually prove be of great importance to condensation in many industrial and engineering applications, such as desalination and electricity generation.

Bibliography

[1] J. W. Rose, *"Dropwise condensation theory and experiment,"* 2002, Procedures of the Institution of Mechanical Engineers, Vol. 216 Part A: Journal of Power and Energy, pp. 115-128

[2] R. Furstner, W. Barthlott, *"Wetting and self-cleaning properties of artificial superhydrophobic surfaces,"* 2005, Langmuir, Vol. 21, pp. 956-961

[3] J. P. O'Sullivan and G. C. Wood, *"The morphology and mechanism of formation of porous anodic films on aluminium,"* 1970, Proc. Roy. Soc. Lond. A., Vol. 317, pp. 511-543

[4] L. Feiyue, L. Zhang, and R.M. Metzger., *"On the Growth of Highly Ordered Pores in Anodized Aluminum Oxide,"* 1998, Chem. Mater., Vol. 10, pp. 2470-2480

[5] S. Wang and L. Jiang., *"Definition of Superhydrophobic States,"* 2007, Adv. Mater., Vol. 19, pp. 3423-3424

[6] E. Bormashenko, T. Stein, G. Whyman, Y Bormashenko, and R. Pogreb., *"Wetting properties of the multiscaled nanostructured polymer and metallic superhydrophobic surfaces,"* 2006, Langmuir Vol. 22, pp. 9982-9985

[7] W. Lee, et. al., *"Nanostructure-Dependent Water-Droplet Adhesiveness Change in Superhydrophobic Anodic Aluminum Oxide Surfaces: From Highly Adhesive to Self-Cleanable,"* 2010, Langmuir Vol. 26, pp. 1412-1415

[8] Wilmshurst, R., *"Heat transfer during dropwise condensation of steam, ethane 1,2 diol, aniline and nitrobenzene,"* 1979, PhD thesis, London University.

[9] Stylianou, S. A., "*Heat transfer during dropwise condensa-*

tion of steam and ethanediol," 1980, PhD thesis, London University.

[10] Young, T., *"An Essay on the Cohesion of Fluids,"* 1804, Philos Trans R Soc London, Vol. 95, pp. 65-87.

[11] J.H. Lienhard IV and J.H. Lienhard V. *A Heat Transfer Textbook*, 4th Edition. Mineola NY: Dover Publications, 2011 pp. 49-84.